

Mammogram Image Enhancement Using Denoising With Segmentation Algorithm Using Global Methods

M.RAMESH, Dr.B.Raveendra Babu

Abstract---In this work a new scheme of active contour modeling with wavelets has been implemented. The scale-space continuation method calculates this snake in a coarsely smoothed image. Further, the result at the coarse scale is used as an initial contour on a finer image and so on, until the negative image resolution is reached. Continuing this method in the wavelet domain detects the lesions in mammographic images more accurately. The reasons for selecting different methods for achieving image enhancement stem from the following observations. All breast images belonging to particular disease invariably exhibit different features, thus necessitating different image enhancement schemes. Fidelity criterion is different for various methods of enhancement.

I. INTRODUCTION

Significant work has been published on the post-processing of compressed images. Most existing post-processing methods are designed to reduce (or to attenuate) the blocking artifacts caused by block discrete cosine transforms based (DCT-based) coding algorithms. Enhancement of compressed images has also been viewed as a restoration problem.

II. EXISTING TECHNIQUES

A. General Steps in Mammographic Lesion Detection Global methods:

Texture analysis [1] allows us to segment the image and classify the segmented regions. These regions can produce parameters for a forthcoming method. The segmentation (or region of interest localization) of the mammograms consists of three parts: preprocessing, “coarse” segmentation and “fine” segmentation. Preprocessing is used to extract the true breast region from the image using thresholding [2] and median filtering. Further algorithms are working only on the extracted region. The “coarse” segmentation calculates various texture parameters (co-occurrence matrix [3], gray level run length, grey level differences and histogram features) in a particular window to create the feature vector. The feature vector is passed to a set of decision trees, which will classify the actual image segment (in which the feature vector is calculated). The decision trees are automatically generated from a set of training images. These training images contain a mass (or lesion) and some surrounding background tissue. The image is segmented using all the decision trees. The output is a vote board where each image segment can

have a vote value between zero and the number of the classifying trees. This vote board is post processed to create a binary mask that will cover regions of interests (suspected locations of lesions). It is treated as an image and adaptive filtering is applied to locate the most suspicious regions. The “fine” segmentation step uses a multiresolution Markov random field [4,5] to improve the preliminary segmentation provided by the “coarse” segmentation.

B. Local Methods

Segmentation is performed on the patches using a combination of dual binarization, Bèzier histograms [6] and a modification of the radial gradient index method to obtain a black-and-white mask. After getting the mask of the lesion candidate, several parameters are calculated. Some of them refer to the shape of the object, compactness; others refer to the texture of the object and its surroundings (e.g. average brightness of the masked area, average brightness of the background, the quotient of these two numbers; and the average variance of the masked and unmasked regions). Based on these parameters, it can be decided whether the patch contains a true lesion or not. Currently human experts evaluate these parameters, but the development of an automatic clustering module is in progress.

In this work, two automatic mammographic lesion detection algorithms namely Fuzzy C means Clustering and Otsu thresholding are compared with the proposed Active Contour model based algorithm.

C. Fuzzy C-means Clustering

Fuzzy C-means Clustering (FCM), also known as Fuzzy ISODATA employs fuzzy partitioning such that a data point can belong to all groups with different membership grades between 0 and 1. FCM is an iterative algorithm. The aim of FCM is to find cluster centers (centroids) that minimize a dissimilarity function.

To accommodate the introduction of fuzzy partitioning, the membership matrix (U) is randomly initialized according to equation (1)

$$\sum_{i=1}^c u_{ij} = 1, \forall j = 1, \dots, n \quad (1)$$

The dissimilarity function which is used in FCM is given Equation (2)

$$J(U, c_1, c_2, \dots, c_c) = \sum_{i=1}^c J_i = \sum_{i=1}^c \sum_{j=1}^n u_{ij}^m d_{ij}^2 \quad (2)$$

$$(3)$$

u_{ij} is between 0 and 1,

c_i is the centroid of cluster i ,

d_{ij} is the Euclidian distance between i_{th} centroid (c_i) and j_{th} data point,

$m \in [1, \infty]$ is a weighting exponent.

To reach a minimum of dissimilarity function there are two conditions. These are given in equation (3) and equation (4).

$$c_i = \frac{\sum_{j=1}^n u_{ij}^m x_j}{\sum_{j=1}^n u_{ij}^m}$$

$$u_{ij} = \frac{1}{\sum_{k=1}^c \left(\frac{d_{ij}}{d_{kj}} \right)^{2/(m-1)}} \quad (4)$$

By iteratively updating the cluster centers and the membership grades for each data point, FCM iteratively moves the cluster centers to the "right" location within a data set.

FCM does not ensure that it converges to an optimal solution. Because of cluster centers (centroids) are initialized using U that randomly initialized (equation 3).

D. OTSU Thresholding

Otsu's method [7] chooses the optimal thresholds by maximizing the inter-class variance with an exhaustive search. It also chooses the threshold to minimize the intra-class variance of the threshold black and white pixels. This method is based on selecting the lowest point between two classes (peaks). Frequency and Mean value is given by equation(5) and equation(6)

$$\text{Frequency: } \omega = \sum_{i=0}^r p(i) \quad P(i) = n_i / n \quad (5)$$

N : total pixel number

$$\text{Mean: } \mu = \sum_{i=0}^r i = P(i) / \omega \quad (6)$$

n_i : number of pixels in level i

Analysis of variance (variance=standard deviation²) is given by equation (7)

$$\text{Total variance: } \sigma_1^2 = \sum_{i=0}^r (i - \mu)^2 P(i) \quad (7)$$

Between-classes variance (δb^2) is given by the variation of the mean values for each class from the overall intensity mean of all pixels as in equation(8).

$$\delta b^2 = \omega_0 (\mu_0 - \mu_t)^2 + \omega_1 (\mu_1 - \mu_t)^2, \quad (8)$$

Substituting $\mu_t = \omega_0 \mu_0 + \omega_1 \mu_1$ in equation (8), equation is given as

$$\delta b^2 = \omega_0 \omega_1 (\mu_1 - \mu_0)^2 \quad (9)$$

where $\omega_0, \omega_1, \mu_0, \mu_1$ stands for the frequencies and values of two classes, respectively.

The criterion function involves inter-classes variance to the total variance and is defined in equation (10)

$$\eta = \delta b^2 / \delta t^2 \quad (10)$$

All possible thresholds are evaluated in this way, and that maximizes η is chosen as the optimal threshold.

III. ACTIVE CONTOUR MODEL

The snake is the simplest form of active contours and is the basic concept of this work. A snake is a contour that can be described as a function $v : [0, 1] \rightarrow \mathbb{R}^2$ with some boundary conditions if required by the situation. The contour is placed on an image $f : \mathbb{R} \rightarrow \mathbb{R}^2$, and it moves towards an optimal position and shape by minimizing its own energy. Fitting active contours to shapes in images is an interactive process. The operator must suggest an initial contour, which is quite close to the intended shape. The contour will then be attracted to features in the image extracted by creating an attractor image.

A. Open and Closed Contours

The contour can be either a closed or an open curve. If the contour is open, one should take care to modify the contour in definition of its energy so that the end-points will not move in the same way as the other points (avoiding the contour dragging itself into itself and vanishing).

B. The Energy Of The Contour

The energy depends on the shape of the contour (internal energy) and on its positioning on the image according to equation (11)

$$E(v, f) = E_{image}(v, f) + E_{int}(v) \quad (11)$$

These energies influence all points along the contour with internal forces and an image force. When all forces are balanced, the total energy is at a minimum.

C. Internal Energy

The internal energy of the contour depends on the shape of the contour and the parameter functions αs_0 and βs_0 and is by equation (12)

$$E_{int} = \int (\alpha(s) |v'(s)|^2 + \beta(s) |v(s)|^2) ds \quad (12)$$

The first term, $|v(s)|^2$, will have larger values if there is a large gap between successive points on the contour and minimizing it will minimize the total length of the contour. The second term $|v(s)|^2$, will be larger where the contour is bending and requires the contour to be as smooth as possible. These terms are weighted by parameter functions, and so α_{s_0} determines the elasticity of the contour, and β_{s_0} determines the rigidity. If α_{s_0} equals zero at some points then discontinuities are allowed there, and where it equals $\beta(s)$ zero, discontinuous curvature such as corners are allowed. To simplify, the parameter-functions will henceforth be regarded as constants.

D. Image Energy

The image energy depends on how the contour is positioned on an attractor image, and it is defined as shown in equation (13)

$$E_{image} = -\int p(v(s), f) ds \tag{13}$$

Where [9] uses an attractor image given by equation (14)

$$p(x, f) = |\nabla f(x)|^2 \tag{14}$$

This attractor image makes the contour attract to edges in the original image.

E. Minimizing The Energy

Minimizing the energy (11) is equivalent to solving the corresponding Euler-Lagrange-equation (15)

$$\alpha.v^m - B.v^{(4)} = -\nabla p(v, f) \tag{15}$$

which simply means that the internal forces shall balance the image forces $\alpha.v^m - \beta.v^{(4)}$

In practice one does not study the contour at all points. Instead, the contour is represented by a vector \bar{v} of control point's v_j . The control points must not be separated by more than a few pixels to prevent the contour from bypassing attractive but small areas in the image. It is the purpose of the elasticity force to keep the control points equidistant.

In the control points v_j the derivatives in (15) can be approximated by finite differences [9], which are given by (16) and (17)

$$v_j^m = v_{j-1} - 2v_j + v_{j+1} \tag{16}$$

Using these expressions equation (5.15) can be written as

$$v_j^{(4)} = v_{j-2} - 4v_{j-1} + 6v_j - 4v_{j+1} + v_{j+2} \tag{17}$$

$$A\bar{v} + \nabla p(\bar{v}, f) = 0$$

Where A is the matrix given by (16) and (17) and insertion of and. A contour can then be calculated with iterations according to Euler's method [90] as shown in equation (18)

$$(I + A)\bar{v}_{k+1} = \bar{v}_k + \nabla p(\bar{v}_k, f) \tag{18}$$

Where \bar{v}_0 is the set of originally suggested control points. One iteration makes each control point move so far in the direction of the image force that it is balanced by the resulting internal forces. Active contours "snakes" can be used to segment objects automatically. The basic idea is the evolution of a curve or curves subject to constraints from the input data. The curve should evolve until its boundary segments the object of interest. This framework has been used successfully by Kass *et al.* [10] to extract boundaries and edges. One potential problem with this approach is that the topology of the region to be segmented must be known in advance. The propagating curve is modeled as a specific level set of a higher dimensional surface. It is a common practice to model this surface as a function of time. So as time progresses, the surface can change to take on the desired shape.

IV. MATHEMATICAL FORMULATION OF LEVEL SETS

Let Ω be a bounded open subset of R^2 , with $d\Omega$ as its boundary. Then a two dimensional image u_0 can be defined as $u_0: \Omega \rightarrow R$. In this case Ω is just a fixed rectangular grid. Now consider the evolving curve C in Ω , as the boundary of an open subset ω of Ω . In other words $\omega \subseteq C$, and C is the boundary of ω ($C = d\omega$).

The main idea is to embed this propagating curve as the zero level set of a higher dimensional function ϕ . The function is defined as follows by equation (19)

$$\phi(x, y, t=0) = \pm d \tag{19}$$

Where d is the distance from (x,y) to $d\omega$ at $t = 0$, and the plus (minus) sign is chosen if the point (x,y) is outside (inside) the subset ω . Now, the goal is to produce an equation for the evolution of the curve. Evolving the curve in the direction of its normal amounts to solving the partial differential equation (20) as given by equation (20)

$$\frac{\partial \phi}{\partial t} = F |\nabla \phi|, \phi(x, y, 0) = \phi_0(x, y)$$

Where the $\{(x,y), \phi_0(x,y) = 0\}$ defines the initial contour, and F is the speed of propagation. For certain forms of the speed function F, this reduces to a standard Hamilton-Jacobi equation. There are several major advantages to this formulation. The first is that $\phi(x,y,t)$ always remains a function as long as F is smooth. As the surface ϕ evolves, the curve C may break, merge and change topology. Another advantage is that the geometric properties of the curve are easily determined from a particular level set of the surface ϕ . For example, the normal vector for any point on the curve C is given by equation (21)

$$\bar{n} = \nabla \phi \tag{21}$$

and the curvature K is obtained from the divergence of the gradient of the unit normal vector to the front as shown in equation (22)

$$K = \text{div} \left(\frac{\nabla \phi}{|\nabla \phi|} \right) = \frac{\phi_{xx}\phi_y^2 - 2\phi_x\phi_y\phi_{xy} + \phi_{yy}\phi_x^2}{(\phi_x^2 + \phi_y^2)^{3/2}} \quad (22)$$

Finally, another advantage is that one is able to evolve curves in dimensions higher than two. The above formulae can be easily extended to deal with higher dimensions. This is useful in propagating a curve to segment volume data.

V. ACTIVE CONTOURS WITHOUT EDGES

As given earlier the curve C can be viewed as the boundary of an open subset ω of Ω (i.e. $C = \partial\omega$). The region ω is denoted by $\text{inside}(C)$ and the region $\Omega \setminus \omega$ by $\text{outside}(C)$. Rather than basing the model on an edge-stopping function, the evolution of the curve is halted with a energy minimization approach.

A simple case is considered where the image u_0 is formed by two regions of piecewise constant intensity. The intensity values are denoted by u_{00} and u_{01} . Furthermore, it is assumed that the object to be detected has a region whose boundary is C_0 and intensity u_{01} . Then $\text{inside}(C_0)$, the intensity of u_0 is approximately $u_{1,0}$, whereas $\text{outside}(C_0)$ the intensity of u_0 is approximately $u_{0,0}$. Then the fitting term is considered by (23)

$$F_1(c) + F_2(c) = \int_{\text{inside}(c)} |u_0(x, y) - c_1|^2 dx dy + \int_{\text{outside}(c)} |u_0(x, y) - c_2|^2 dx dy \quad (23)$$

where C is a curve, and the constants c_1, c_2 are the averages of u_0 inside and outside of C respectively. From the figure 5.1, if the curve C is outside the object, then $F_1(C) > 0, F_2(C) \approx 0$. If the curve is inside the object, then $F_1(C) \approx 0, F_2(C) > 0$. If the curve is both inside and outside the object, then $F_1(C) > 0; F_2(C) > 0$. However, if the curve C is exactly on the object boundary C_0 , then $F_1(C) \approx 0, F_2(C) \approx 0$, and the fitting term is minimized.

Some regularization terms are added as in the Mumford-Shah segmentation model [99]. Therefore attempts are made to minimize the length of the curve and the area of the region inside the curve. So the energy function E is given by equation (24)

$$E(C, c_1, c_2) = \mu \cdot \text{Length}(c) + \nu \cdot \text{Area}(\text{inside}(c)) + \lambda_1 \int_{\text{inside}(c)} |u_0(x, y) - c_1|^2 dx dy + \lambda_2 \int_{\text{outside}(c)} |u_0(x, y) - c_2|^2 dx dy \quad (24)$$

where $\mu \geq 0, \nu \geq 0, \lambda_1 > 0, \lambda_2 > 0$ are fixed parameters. So the goal is to find C, c_1, c_2 such that $E(C, c_1, c_2)$ is minimized.

Mathematically, it is to solve $\sum_{i=1}^c u_{ij} = 1, \forall j = 1, \dots, n$

$$F_1(C) > 0, F_2(C) \approx 0 \quad F_1(C) \approx 0, F_2(C) > 0$$

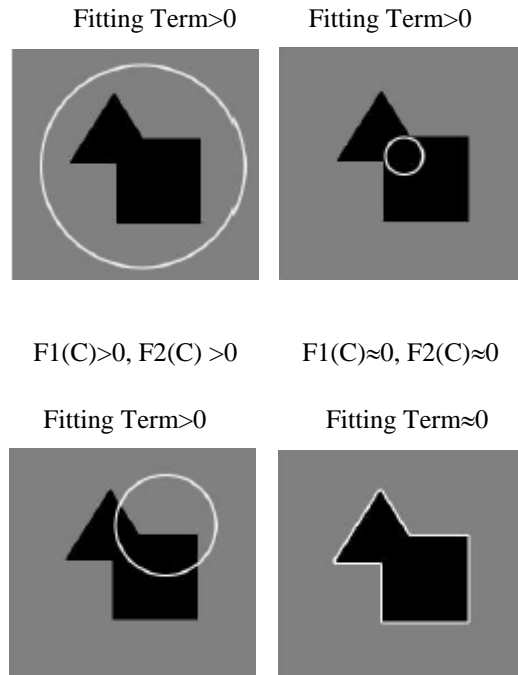


Fig 1 All possible cases in position of the curve

This problem can be formulated using level sets as follows. The evolving curve C can be represented by the zero level set of the signed distance function ϕ as in (1). So the unknown variable C is replaced by ϕ . Now the Heaviside function H is considered, and the Dirac measured as shown in equation (25)

$$H(z) = \begin{cases} 1 & \text{if } z \geq 0 \\ 0 & \text{if } z < 0 \end{cases}, \quad \partial(z) = \frac{d}{dz} H(z) \quad (25)$$

The length of $\phi = 0$ and the area of the region inside ($\phi = 0$) can be rewritten using these functions. The Heaviside function is positive inside the curve and zero elsewhere, so the area of the region is just the integral of the Heaviside function of ϕ . The gradient of the Heaviside function defines the curve, so integrating over this region gives the length of the curve.

VI. SEGMENTATION ALGORITHM

Energy Minimization Algorithm with Jacobi Method is given as:

Initialize ϕ^0 by $\phi_0, n = 0$

for fixed number of iterations do

 Compute $c_1(\phi^n)$ and $c_2(\phi^n)$

Estimate forward differences of ϕ^{n+1} using Jacobi method

Compute ϕ^{n+1}
End

Using the energy minimization approach, the desired segmentation is achieved in digital mammogram images.

VII. EXPERIMENTAL RESULTS

Images from the MIAS (Mammographic Image Analysis Society) database with lesions have been tested. Fig. 3(a) shows a sample mammogram image, Figure. 3(b-d) shows the detected clusters using FCM clustering, Otsu thresholding and Active contour models respectively.

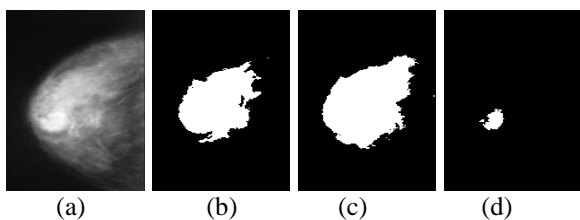


Fig. 3(a) a sample mammogram image (b) the detected clusters using FCM clustering, (c) Otsu thresholding and (d) Active contour models

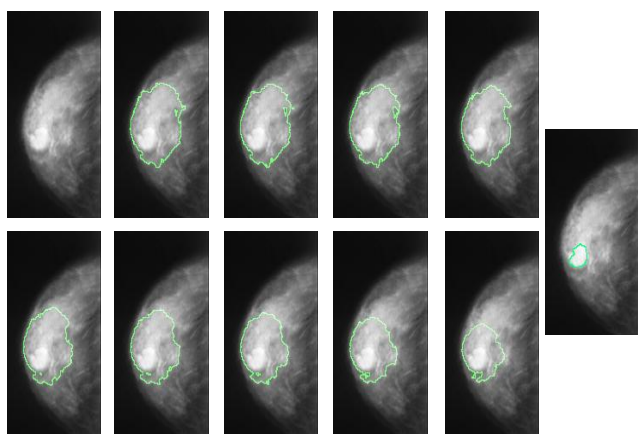


Fig 4. Images from the MIAS (Mammographic Image Analysis Society) database with lesions has been tested

Figures 3(d) and (4) shows the result where the clusters are detected with clear boundaries using active contour model with wavelets than the existing techniques.

Table 1 The segmentation error of these methods

Number of pixels in the image	Error (%)		
	Figure (b)	Figure (c)	Figure (d)
4096	7.81	11.91	1.51

I. TABLE 1 SHOW THAT THE ERROR DUE TO SEGMENTATION OF THE REGION OF INTEREST IS LESS WITH PROPOSED METHOD WHEREAS IT REACHES ITS MAXIMUM VALUE OF 11.91 FOR OTSU THRESHOLDING METHOD.

VIII. CONCLUSION

In the existing segmentation techniques there is much to upgrade and there are many methods to find but the round of possibilities of the new, fast and efficient methods up rise is getting smaller and so the methods with the bigger computing difficulty again [12,13] are arrived at. The active contour methods have many advantages and acquisitions to the image segmentation. However there are some disadvantages to which it can be counted that the fact of their dependency on the initial points of the contour, type of the image and the above mentioned computing difficulty as well. By the use of less accurate but satisfactory methods, it is possible to lower the computing difficulty, the choice of the initial points of the contour can be automated but it can be said that in the last years the trend is to use the interactivity with the user [14].

The principle advantage of the snake is that the image data (the initial estimate) desired contour properties and knowledge-based constraints are integrated into a single extraction process. The presence of an edge depends not only on the gradient at a specific point but also on the spatial distribution of the gradient. Snakes incorporate this global view of edge detection by assessing continuity and curvature combined with the local edge strength to determine an edge.

REFERENCES

- [1] Kass M., Witkin A., and Terzopoulos D. "Snakes: Active contour models", International Journal of Computer Vision, vol 1(4), pp. 321-331, 1998.
- [2] Laine A., Fan J., and Yang W., "Wavelets for contrast enhancement of digital mammography", IEEE Engineering in Medicine and Biology Magazine, vol. 14, no.5, pp. 536-550, 1995.
- [3] Johns P.C and M.J Yaffe,"X-ray Characterization of normal and neoplastic breast tissues", Phys.Med. Biol., vol. 32, no. 6, pp. 675-695, 1987.
- [4] M. Vetterli and J. Lebrun, "Balanced multiwavelets theory and design", IEEE Trans. Signal Processing. vol. 46, pp. 1119-1124, 1998.
- [5] Vetterli M., "Filter banks allowing perfect reconstruction", Signal processing, vol. 10, no. 3, pp. 219-244, 1986.
- [6] Andersson I, Nyström L "Mammography screening", J National Cancer Institution. vol. 87, pp. 1263-1264, 1995.
- [7] Ivan W.Selesnick, "Interpolating Multiwavelet Bases and Sampling Theorem", vol: 47, Issue: 6, pp.1615-1621, 1998.
- [8] Westelius C. J., "AVS for beginners", International report, Computer Vision Lab., Linköping University.
- [9] Westerink P.H., Boekee D.E., Biemond J., and J.W.Woods, "Subband coding of images using vector quantization", IEEE Transaction Commun, vol. 36, no.6, pp. 713-719, 1988.



ISSN: 2277-3754

ISO 9001:2008 Certified

International Journal of Engineering and Innovative Technology (IJET)

Volume 3, Issue 1, July 2013

- [10] Donoho D. L., "De-noising by softthresholding", IEEE Transactions on Information Theory, vol.41 (3): pp.613-627, 1995.
- [11] Woods J.W. and S.D.O'Neil., "Sub band coding of images", IEEE Transaction Acoust, Speech, signal processing, vol. 34, no.5, pp.1278-1288, 1986.
- [12] Xia X.G., J. S. Geronimo, D. P. Hardin, and B.W. Suter, "Design of prefilters for discrete multiwavelets transforms", IEEE Transaction Signal Processing, vol. 44, pp. 25-35, 1996.
- [13] Good WF, Sumkin JH, Dash N, et al., "Observer sensitivity to small differences: a multipoint rank order experiment", AJR; vol.173, pp. 275-27, 1999.
- [14] Yamada Y., Tazaki S., and R. M. Gray," Asymptotic performance of block quantizes with difference distortion measures", IEEE Transaction Inform. Theory, vol. 26, pp. 6-14, 1980.

AUTHOR(S) BIOGRAPHY

M.Ramesh obtained his Masters in Computer Science and Technology from Andhra University, Visakhapatnam. He is now working as Associate Professor in the Department of Information Technology, RVR & JC College of Engineering, Guntur, India. He has 15 years of teaching experience. His area of research interest includes Image Processing, Data Mining and Multimedia Processing.

Dr.B.Raveendra Babu obtained his Masters in Computer Science and Engineering from Anna University, Chennai. He received his Ph.D. in Applied Mathematics at S.V University, Tirupati. He is now working as Professor in the Department of Computer Science and Engineering, VNR VJIET, Hyderabad. He has 27 years of teaching experience. He has more than 55 International and National publications to his credit. His area of research interest includes Data Mining, Image Processing, Pattern Analysis and Information Security.